

Porosity Control During Preparation of Bronze Filter Materials by Powder Metallurgy

Saleh K. Jabur
Engineering College
University of Basrah

Adnan S. Jabur
Engineering College
University of Basrah

Abstract

The ability to achieve close control of porosity and pore size is the main reason that filters are produced by powder metallurgy. This study was performed using bronze alloy powder (Cu-7.5%Sn- 0.1%Fe-0.3%Pb-0.15%Zn). The samples were prepared by two methods : (1) cold die compacting at different particle size, compacting pressure, sintering time, and sintering temperature, and (2) loose powder sintering. The compacts were sintered under controlled atmosphere. After surface preparation of the samples, the microstructure was used to compute the apparent porosity. It was found that the (Loose Powder Sintering) method is optimum method to produce highly porous materials with (~59%) porosity when selecting the proper conditions. The porosities obtained using cold die compaction are ranging between (5-41%) and sintered density ranging between (58.6-94.3%) of the theoretical mean density of the starting materials.

Keywords: Powder Metallurgy, Porous Materials and Porosity.

المستخلص

أن السبب الرئيس في استخدام المرشحات المصنعة من مساحيق المعادن هوقابلية الحصول على نسبة مسامية مسيطر عليها. الدراسة أنجزت باستخدام سبيكة برونز على شكل مسحوق. تم تحضير النماذج بطريقتين: (1) كبس على البارد عند ضغوط كبس مختلفة وحجم حبيبات المسحوق مختلفة (Cu-7.5%Sn- 0.1%Fe-0.3%Pb-0.15%Zn) كذلك زمن وحرارة التلييد مختلفين, (2) الطريقة الأخرى لتحضير العينات هي Loose Powder Sintering. المكبوسات لبدت في جو مسيطر عليه. بعد تحضير السطح, العينات عولجت لحساب المسامية الظاهرية. لقد وجد أن الطريقة الأفضل لإنتاج المواد ذات المسامية العالية حوالي (59%) هي (Loose Powder Sintering) عند استخدام الظروف الملائمة. المسامية التي تم الحصول عليها باستخدام كبس على البارد والتلييد تتراوح بين (5-41%) والكثافة تتراوح بين (58.6- 94.3%) من الكثافة النظرية للمادة الخام.

1. Introduction

Powder metallurgy is the most common method to produce porous metallic products, where the level of porosity and the size distribution of pores are controlled. The three groups of porous materials produced commercially differ primarily in their porosity. These include [1];

1. Metallic materials in which the porous structure serve as reservoir for lubricant, such as self-lubricating bearings.
2. Metallic materials which has a controlled rate of permeation of fluids (liquid or gas) through the porous structure and which serve primarily as filters.
3. Metallic materials which contain a very high internal surface area and serve as porous electrodes for batteries and fuel cell.

A rigid, permeable structure can be created using P/M by forming a network of sintered powder particles and interconnected pore channels. Using similar manufacturing equipment and technology as structural P/M components, porous P/M materials are normally sintered to densities between 25% and 85% of theoretical mean density [2]. By varying the compaction pressure, particles properties, sintering temperature and time, a range of porosity could be achieved [3]. Materials can be selected from wide varieties depending on the combination of application requirements and economics. The porosity is determined by the powder particle shape, the particle size, size distribution, surface texture, and other powder characteristics that depend on the material processing method. The four most common porous P/M materials are bronze, stainless steel, nickel, and nickel-base alloys [4].

The aim of this work was to study the effect of the following four parameters on the porosity of the sintered bronze filter compacts. These parameters are: compaction pressure, sintering temperature, sintering time and powder particle size.

Two methods were used to produce filter materials; loose powder sintering and cold die compaction.

2. Experimental procedures

The bronze powder was prepared by filing process, which gave a different particle sizes with an irregular particle shape as shown in the figure (1). The composition of the bronze powder was achieved by analysis the alloy using X-ray fluorescent spectrometer with specification of: high resolution peltier cooled Si-PIN detector, 40 KV tube voltage and Ag

target. Different particle sizes were obtained after sieving of the prepared powder for (15 min.) as shown in Figure (2). 0.7%wt of synthetic wax as a binder was mixed with the powder to promote powder compaction and ejection from the die and obtaining adequate green strength to reduce die wall friction [5]. The compaction die consisted of cylindrical bushing as cavity to fill with powder and two punches; upper and lower which were used to apply the load by manual operation press.

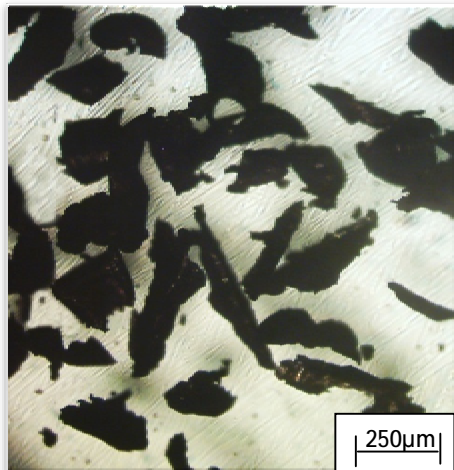


Figure (1). Optical micrograph showing powder particle shape.

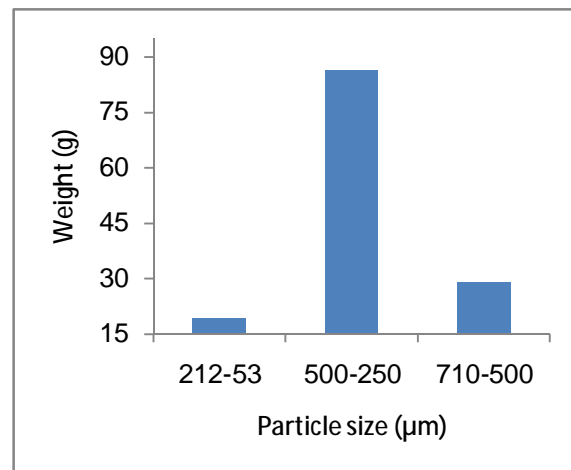


Figure (2). Bar chart of particle size distribution.

After compaction, the samples were sintered at specified temperatures (700, 800, 850, and 900) $^{\circ}\text{C}$ under argon atmosphere. The sintering furnace is shown in Figure (3). The compacts were pre sintered at a temperature of (450 $^{\circ}\text{C}$) for (20 min) in order to remove the lubricant and to avoid sample blistering [6].

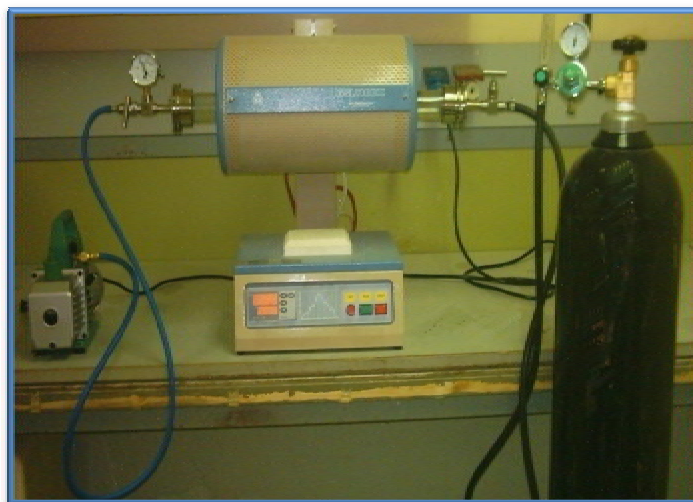


Figure (3). Vacuum tube furnace.

The following samples were used:

a) Compacting pressure effect:

Four samples with a particle size of (250-500 μm), were compacted under (200,300,400 and 500 MPa) pressures and sintered at 900 °C for 30 min under controlled atmosphere (Argon gas).

b) Particle size effect:

Three samples with different particle size ranges (53-212,250-500 and 500-710 μm), were compacted under 300 MPa pressure and sintered at 900 °C for 30 min under controlled atmosphere (Argon gas).

c) Sintering time effect:

Four samples with a particle size of (250-500 μm), were compacted under 300 MPa pressure and sintered at 900 °C for (15, 30, 45, 60) min under controlled atmosphere (Argon gas).

d) Sintering temperature effect:

Four samples with a particle size of (250-500 μm) were compacted under 300 MPa pressure and sintered at (700, 800, 850, 900) °C for 30 min under controlled atmosphere (Argon gas).

e) Particle size effect under Loose powder sintering:

Particle size ranges (53-212,250-500,500-710 μm) were studied. This process involved pouring of loose powder (non compacted) into small steel dishes, then this dishes was inserted into the sintering furnace. The sintering temperature was 900 °C for 30 min under controlled atmosphere (Argon gas).

The following steps applied to testing the samples experimentally according to ASTM C373 [7]:

- i. Dry the test samples to constant mass by heating in an oven at 150°C (302°F), followed by cooling. Determine the dry mass, D , to the nearest 0.01 g.
- ii. Place the samples in a pan of distilled water and boil for 5 h, taking care that the samples are covered with water at all times.
After the 5-hr boil, allow the samples to soak for an additional 24h.
- iii. After impregnation of the test samples, determine to the nearest 0.01 g the mass, S , of each sample while suspended in water.

- iv. After ejecting the samples from water, use cotton cloth to remove all excess water from the surface, and determine the saturated mass, M , to the nearest 0.01 g.

The following calculation can do[7]:

1. Calculate the exterior volume, V , in cubic centimeters, as follows:

$$V = M - S \quad (1)$$

2. Calculate the volumes of open pores V_{op} and impervious portions V_{Ip} in cubic centimeters as follows:

$$V_{op} = M - D \quad (2)$$

$$V_{IP} = D - S \quad (3)$$

3. The apparent porosity, P , expresses, as a percent, the relationship of the volume of the open pores of the sample to its exterior volume. Calculate the apparent porosity as follows:

$$P = \left[\frac{M-D}{V} \right] * 100 \quad (4)$$

4. The bulk density, B , in grams per cubic centimeter, of a sample is the quotient of its dry mass divided by the exterior volume, including pores. Calculate the apparent density as follows:

$$B = \frac{D}{V} \quad (5)$$

3. Image processing

The samples were mounted and ground using emery paper of grades (320, 400, 1000, and 1200). The polishing process was carried out using aluminapowder suspension of (0.5 μm) particle size [8]. The microstructure images were taken using an optical microscope and digital camera, and then they were treated by the (Photoshop CS2 and Image J) to estimate the apparent porosity computationally, which will be compared with the experimental data.

1. Image Treatment

a. Selection Stage

The aim of this stage is to select a suitable region. This step can be done in the following steps:

- The picture opens with "Photoshop CS2" program.
- Suitable area select from the picture using "Rectangular Marquee Tool M" from the tool list.
- New picture saves as a JPG type (figure 4b).

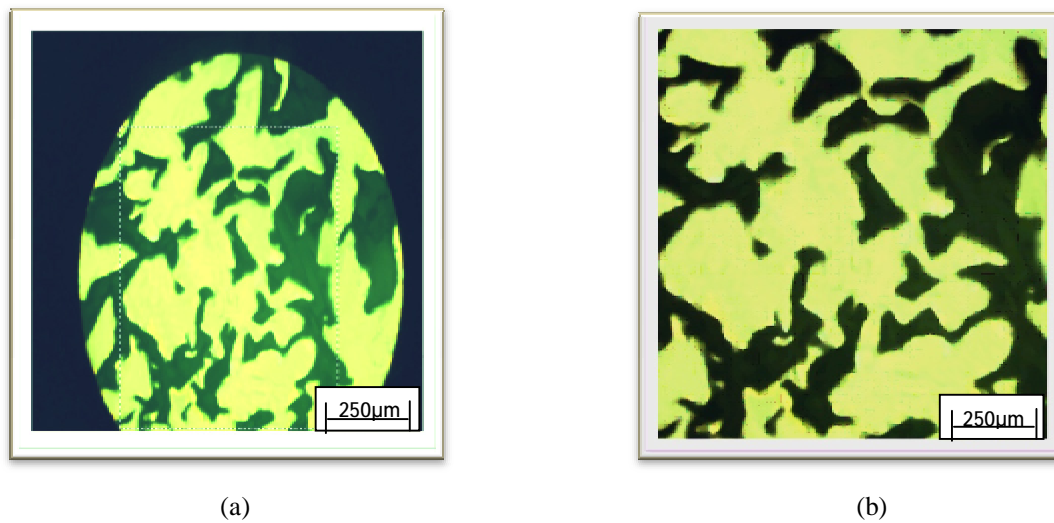


Figure (4). Selection Stage.

b. Porosities Planning

- The new picture opens with Photoshop CS2 program, and improving its contrast and level by
- pressing on Adjustment then Auto Contrast from the image list.
- The porosities plan by "Brush Tool" (B) from the tool list.

New picture saves as JPG type (figure 5).

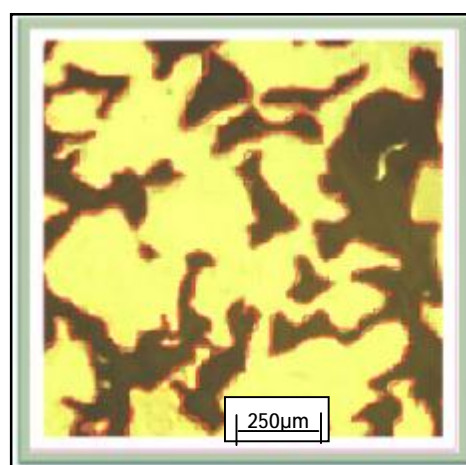


Figure (5). Porosities Planning.

c. Image Threshold

- The new picture opens with Photoshop CS2 program.
- The images changes to black and white colors by pressing on Adjustment then threshold command from the image list with a suitable level depending on the image nature, the final requirement, and the operator experience.
- Pressing on Noise then Dust &Scratches from the filter list and choosing a suitable radius value for the image. Figure (6) shows the all steps of this stage.



Figure (6). Threshold stage, (a) Threshold step, (b) Dust and scratches step.

2. The Apparent Porosities Estimation

Using the Image J program, the estimation of the apparent porosities of sintered compacts can be done by these following steps:

- Opening final picture with Image J program and processing this picture as follows:
- Process → Binary → Threshold.
- Image → Adjust → Threshold → Black & White.
- Analysis → Analysis of particles.

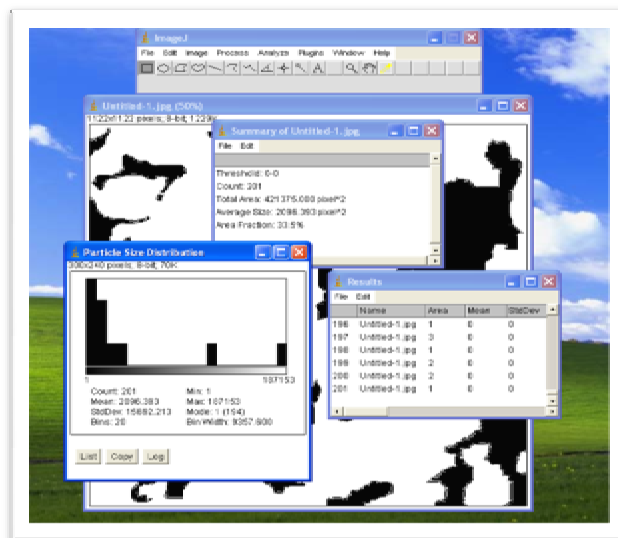
The program measures and scans all the picture and gives results box, this involves:

- Count of particles (pores)
- Total area of particles (pores)
- Average size of particles (pores)
- Area fraction (which represents the apparent porosity of sample).



(a)

(b)



(c)

Figure (7). Estimation process of porosity, (a) Threshold, (b) black&White, (c) Analysis particles.

The shrinkage percentage can be determined from the following equation [8]:

$$\text{Shrinkage (or growth) \%} = \frac{\text{Change in Length}}{\text{Sintered Length}} \times 100 \quad (6)$$

4. Results and discussion

4.1 The Effect of Compacting Pressure

Figure (8) shows the variation of the green density of compacts with compacting pressure. It is clear that the green density increased with increasing compacting pressure, which is due to decreasing the spacing between particles by particles movement and plastic deformation. The highest green density of (7.15 g/cm^3) was obtained at a compaction pressure of 500 MPa. Apparent porosity which is the amount of pores in the volume of sintered compact is shown in Figure (9) as a function of compacting pressure. It is clear that the apparent porosity decreased with increasing the compacting pressure due to the reduction in the number and size of pores. Figure (12) shows this variation.

In Figure (10), the water adsorption of the sintered compacts decreased with increasing the compacting pressure. The large drop of water adsorption appeared as linear function with compacting pressure until 400 MPa. However, the volume fraction of pores reaching steady state. Figure (11) shows the variation of the bulk density of sintered compacts with compacting pressure. It increased with increasing compacting pressure due to increasing contact regions which enhance necking and diffusion between particles during sintering.

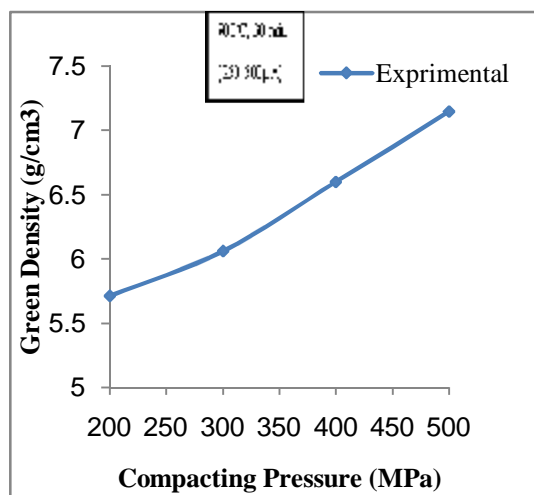


Figure (8). Green density as a function of compacting pressure .

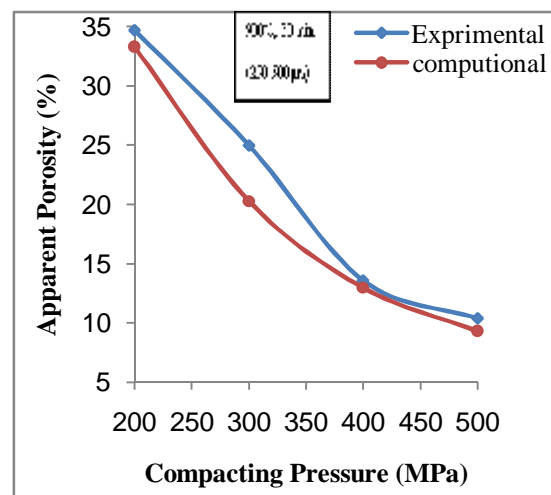


Figure (9). Apparent porosity as a function of compacting pressure .

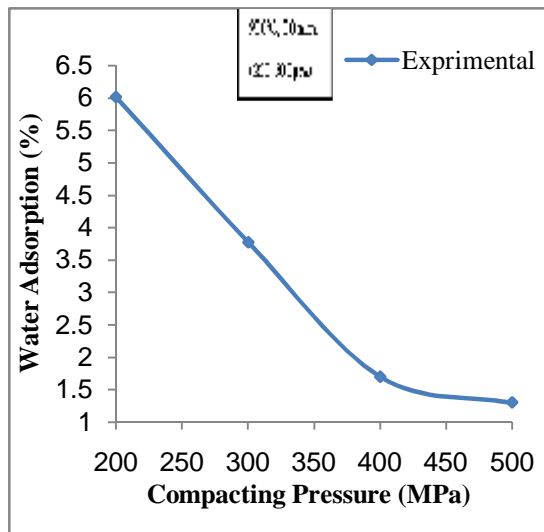


Figure (10). Water adsorption as a function of compacting pressure.

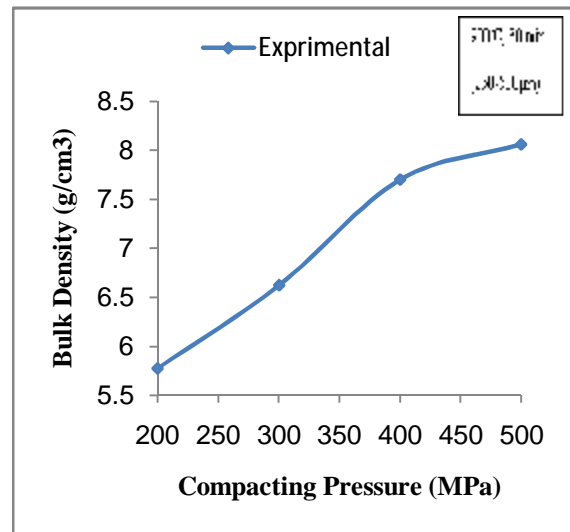
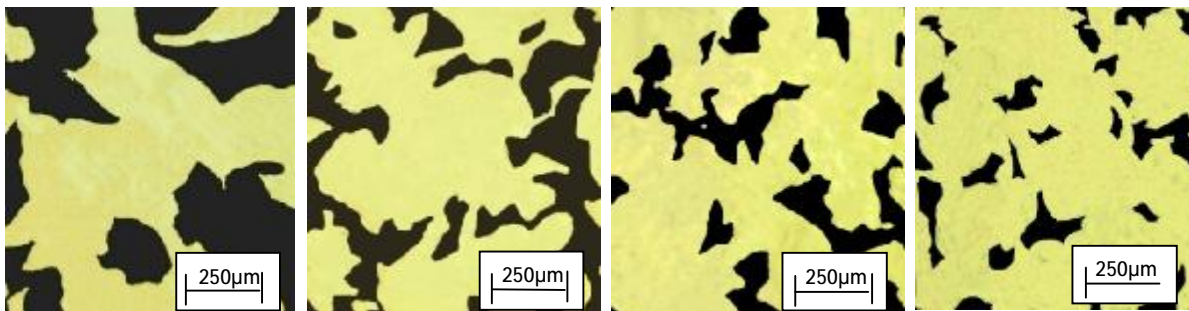


Figure (11). Bulk density as a function of compacting pressure.



(a)

(b)

(c)

(d)

Figure (12). The microstructural images of sintered samples with different compacting pressures; (a) 200 MPa (b) 300 MPa (c) 400 MPa (d) 500 MPa.

4.2 The Effect of Sintering Time

From Figure (13), it was found that the apparent porosity of compacts decreased linearly with the sintering time. The increasing of sintering time process at high temperature (900 °C) causes particles growth which relatively leads to close the voids between particles. Figure (17) shows this variation. Water adsorption behavior resembles the porosity behavior with sintering time as shown in Figure (14).

Variation of bulk density with sintering time at 900 °C of sintering temperature is shown in Figure (15). It is clear that bulk density of sintered compacts increased with sintering time up to (45 min.) reaching a steady state. Figure (16) presents the influence of the sintering time on the shrinkage of sintered samples. It is clear that, the shrinkage percent increased with increasing the sintering time.

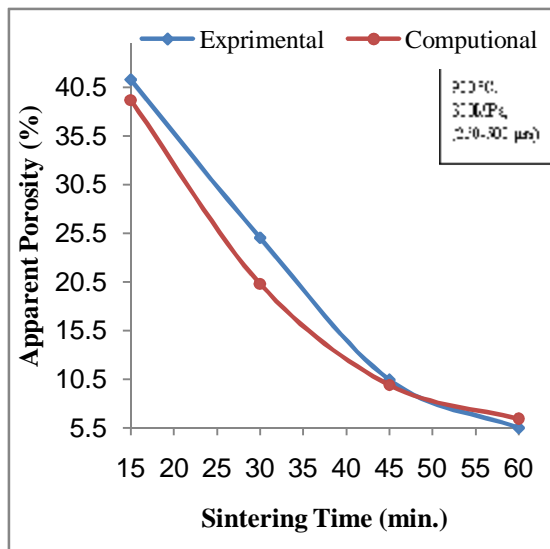


Figure (13). Effect of sintering time on apparent porosity.

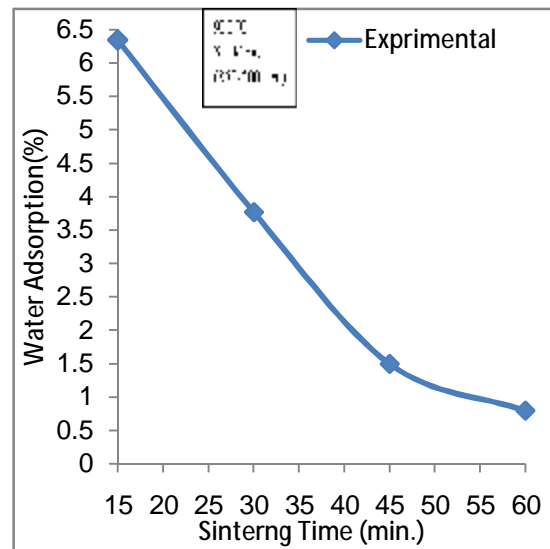


Figure (14). Relationship between water adsorption and sintering time.

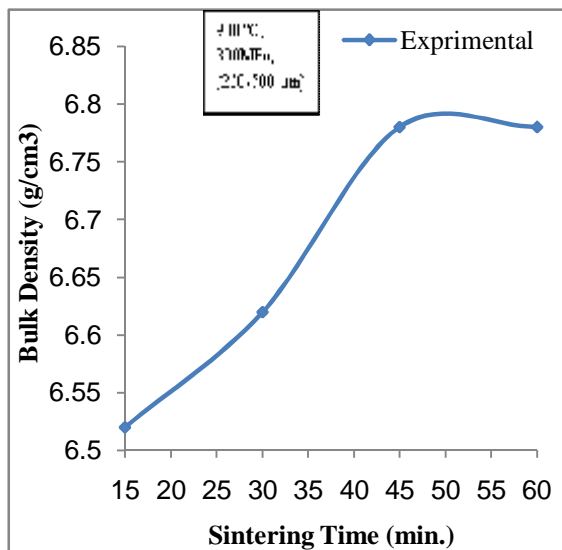


Figure (15). Effect of sintering time on bulk density of prepared alloy.

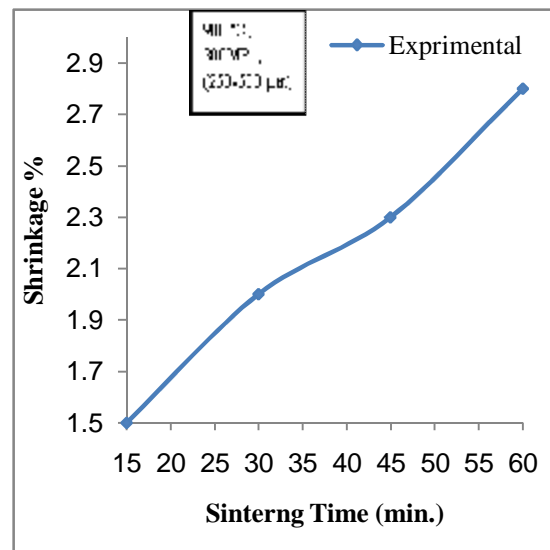


Figure (16). Shrinkage of bronze powder compacts as a function of sintering time.

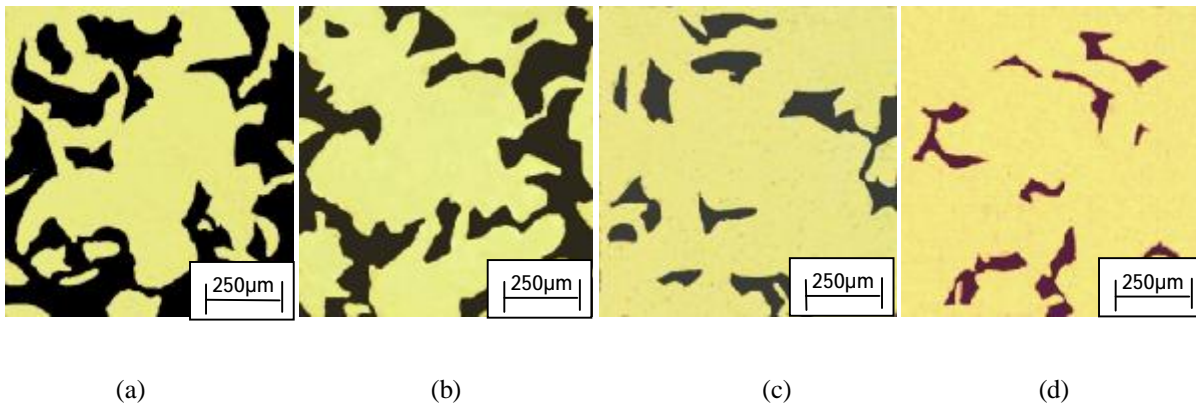


Figure (17). The microstructure images of samples sintered for, (a) 15min. (b) 30min. (c) 45min. (d) 60 min.

4.3 The Effect of Sintering Temperature

Figure (18) shows the effect of sintering temperature on the apparent porosity of sintered samples. It can be seen that the porosity of the sintered compacts decreased with increasing the sintering temperature because of growth and swelling of particles which leads to close the voids between them. Figure (22) shows this variation.

Also, the water adsorption as a function of the sintering temperature is shown in the Figure (19). It decreased with increasing the sintering temperature. Bulk density as a function of sintering temperature is shown in Figure (20). It increased with low rate up to (850 °C), so it showed a rapid increasing which may be due to the reduction of pore size and number. Figure (21) shows the influence of sintering temperature on the shrinkage percentage of sintered compacts. It shows that the shrinkage percentage increased with increasing sintering temperature.

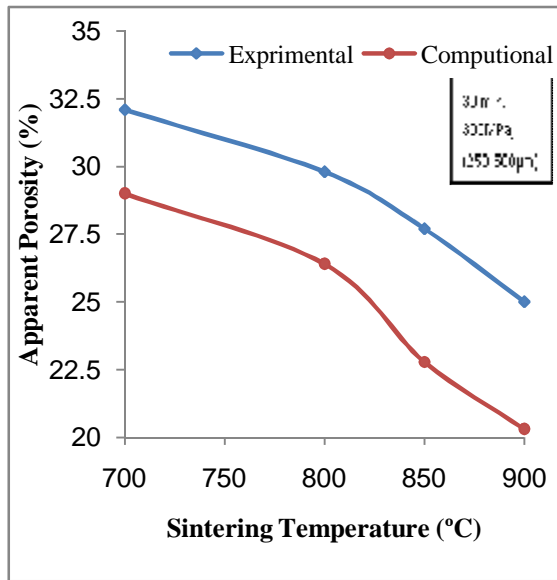


Figure (18). Effect of sintering temperature on apparent porosity.

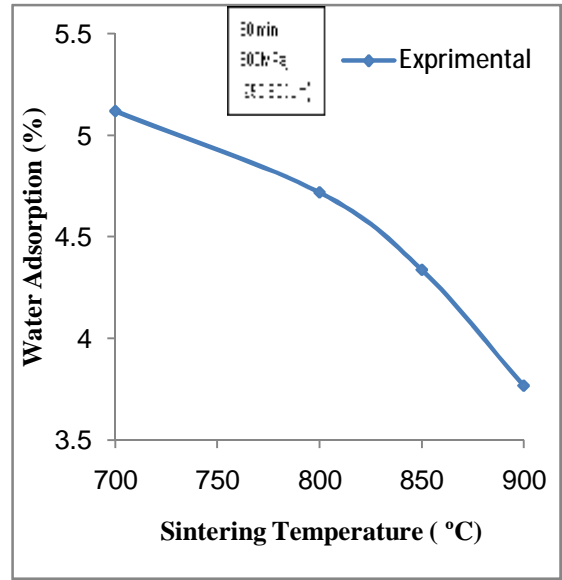


Figure (19). Water adsorption as a function of sintering temperature.

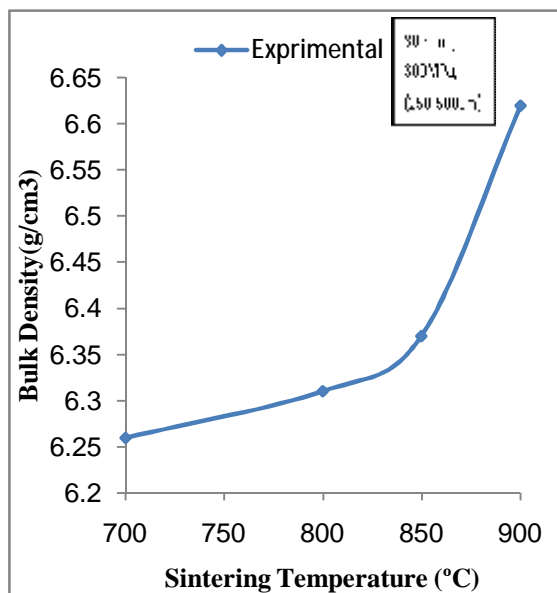


Figure (20). Effect of sintering temperature on the bulk density of prepared alloy.

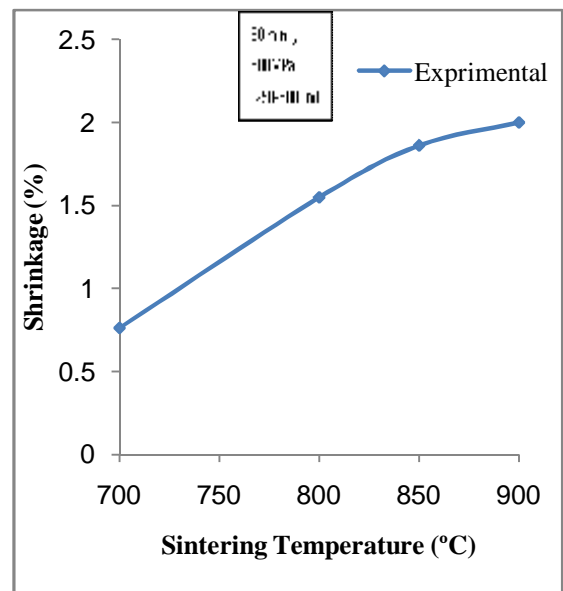


Figure (21). Shrinkage of bronze powder compacts as a function of sintering temperature.

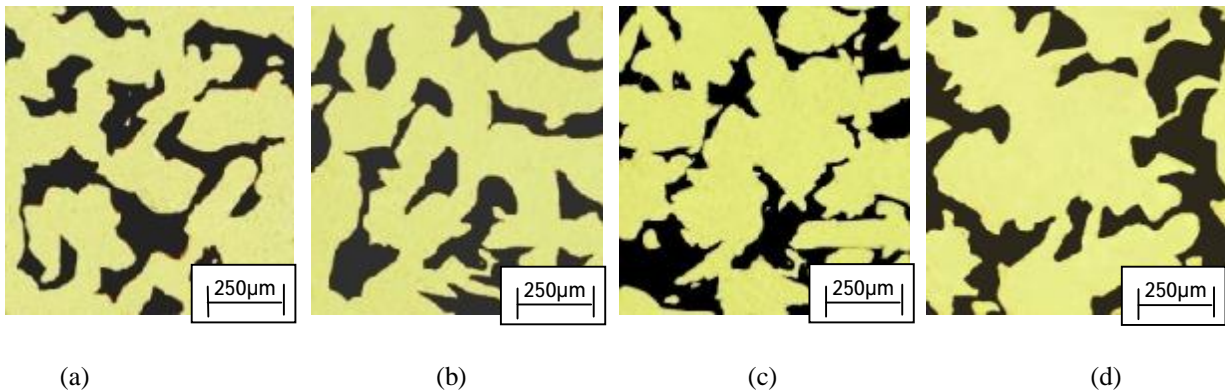


Figure (22) .The microstructure images of samples sintered at, (a)700 °C (b) 800 °C (c) 850 °C (d) 900 °C, for (30 min).

4.4 The Effect of Powder Particle Size

As shown in the Figure (23) the apparent porosity of sintered samples increased with increasing the particle size of the powder. This is due to the number of contacts in the fine particles is larger than coarse particles which causes the increasing of sintering rate, reducing of apparent porosity and increasing of bulk density (Figure 25).

Figure (26), also shows these changes. The relationship between the water adsorption and powder particle size is shown in the Figure (24). From this figure, it is clear that the water adsorption increased with increasing the powder particle size.

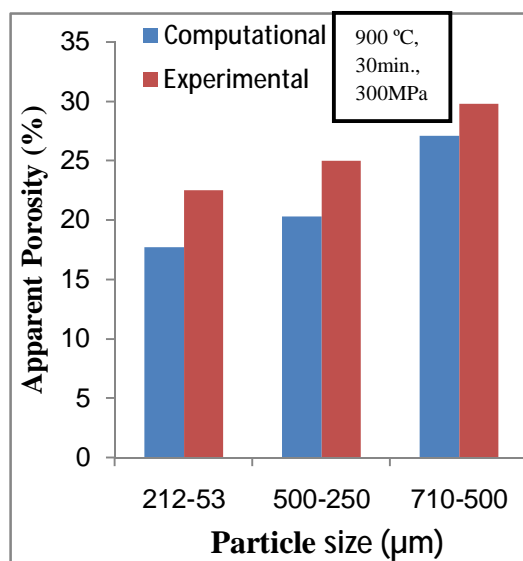


Figure (23). Effect of powder particle size on the apparent porosity.

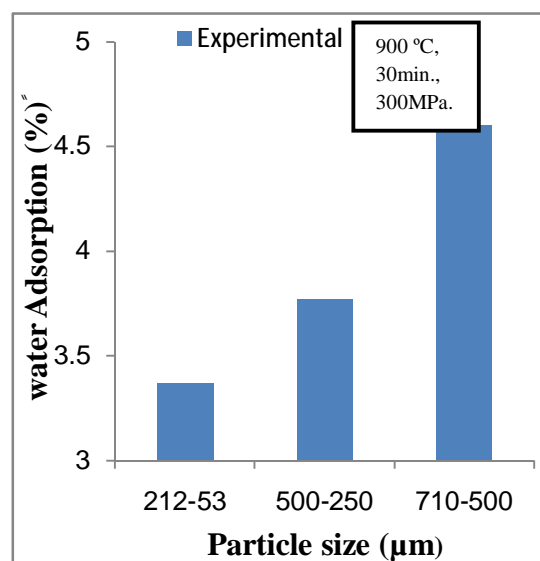


Figure (24).Water adsorption as a function of the powder particle size.

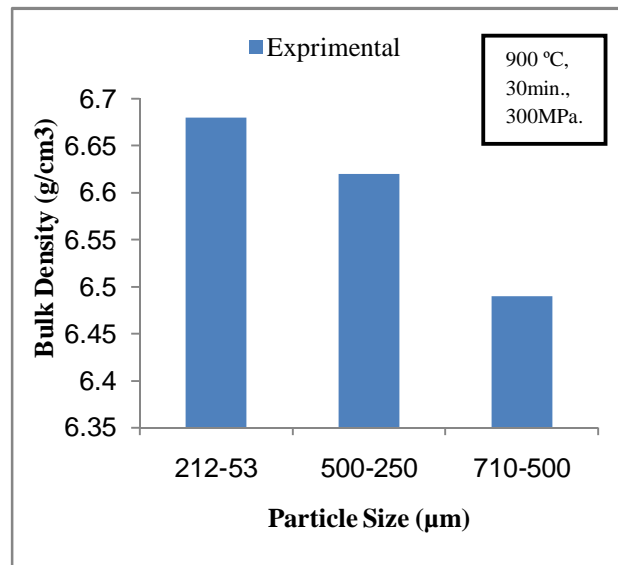


Figure (25). Effect of powder particle size on the bulk density of prepared alloy.

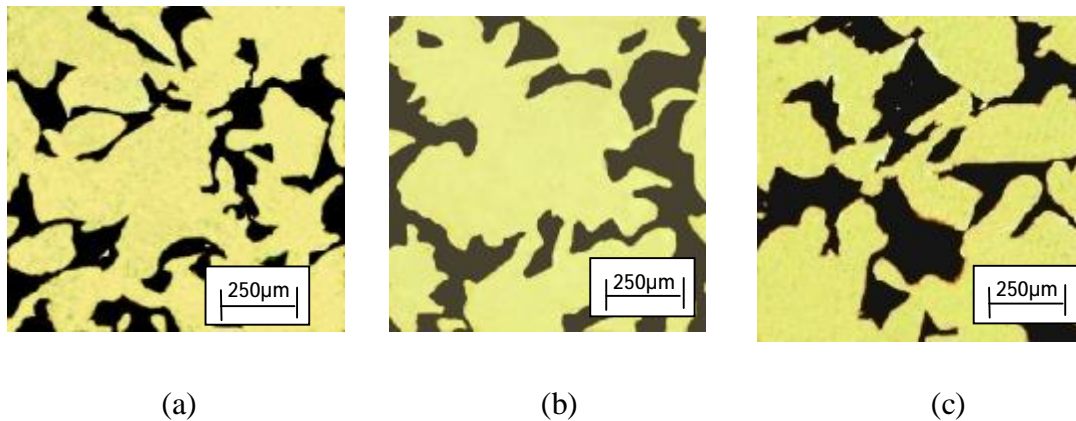


Figure (26) .The microstructure images of samples prepared at different particle sizes (a) (53-212 μm) (b) (250-500 μm) (C) (500-710 μm).

4.5 The Effect of Loose Powder Sintering

Here, the effect of particle size on the apparent porosity, water adsorption and bulk density of loose sintered samples (Figures 27, 28, 29 and 30) are similar to that in Figures (23, 24, 25 and 26). These behaviors can also be explained by the same way. But when comparing between loose sintered and compacted sintered samples behaviors, the formers developed higher apparent porosity and water adsorption and lower bulk density.

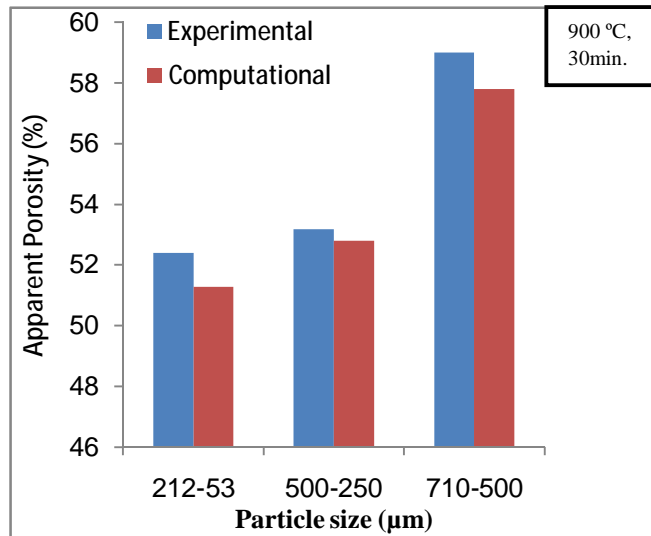


Figure (27). Effect of powder particle size on the apparent porosity.

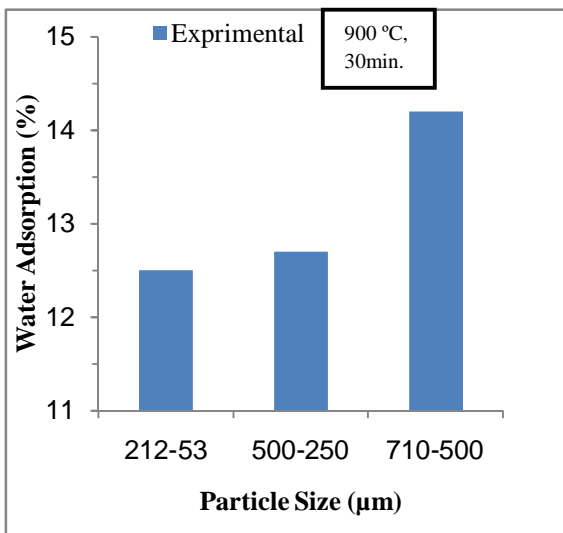


Figure (28). Water adsorption as a function of powder particle size.

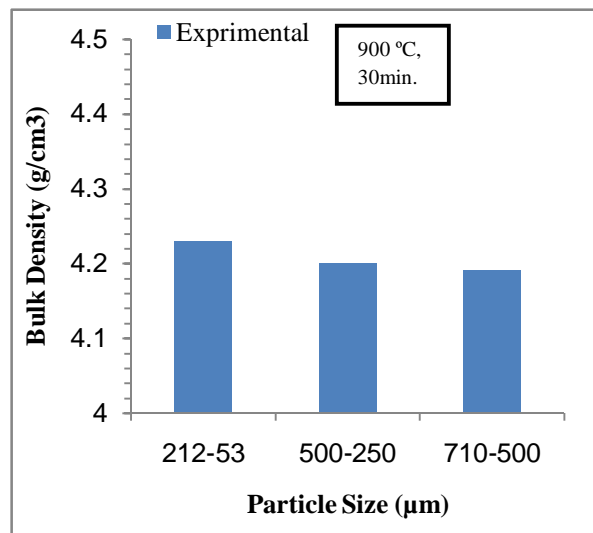


Figure (29). Effect of powder particle size on the bulk density of prepared alloy.

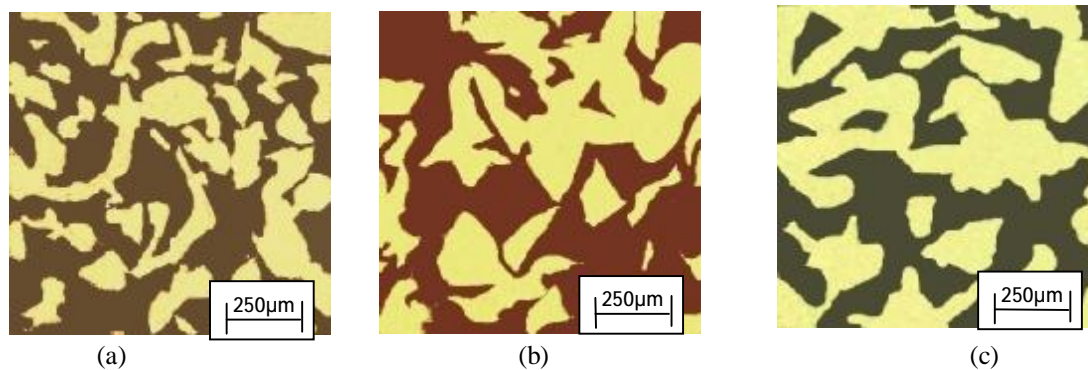


Figure (30). The microstructure images of samples prepared by loose powder sintering (a) 53-212 μm (b) 250-500 μm (c) 500-710 μm .

5. Conclusions

1. Loose Powder Sintering method is an optimum method to produce highly porous materials with porosity percent of about (59%) with proper conditions.
2. The higher sintering time was undesired because it reduced the porosity value to about (5.5%).
3. Using powder particles with a flake, acicular and irregular shape was proper to prepare the bronze filter materials with porosities ranging between (5-59%).

6. References

- [1] M.Can and A.B.Etemoglu, "Porosity Measurement of Stainless Steel Filters Produced by Electric Discharge Technique", Powder Metallurgy International, Vol.17, PP340-349, No.5, 2004.
- [2] M.Eisenmann, "Porous PM Technology", ASM Handbook, Vol.17, 2000.
- [3] D. Poquillon, J. Lemaitre, V. Baco-Carles, Ph. Tailhades, J. Lacaze, "Cold compaction of iron powders—relations between powder morphology and mechanical properties Part I: Powder preparation and compaction", Powder Technology, Vol.126, PP65-74, 2002.
- [4] L.Albano-MÜLLER, "Filters Elements of Highly Porous Sintered Metals", Powder Metallurgy International, Vol.14, No.2, 1982.

- [5] I.Vida-Simiti, N.Jumate and T.Bolog, "Experimental Research of Sintered Porous Materials of Bronze Powders ", Journal of Optoelectronics and Advanced materials, Vol.8, No.2, PP716-719, April 2005.
- [6] D. Garg, K. Berger, D. Bowe, and J. Marsden," Effect of Atmosphere Composition on Sintering of Bronze:, Gas Interactions in Non Ferrous Metal Processing, Minerals, Metals and Materials Society, PP17-26, 1996.
- [7] ASTM C373, "Standard Test Method for Water Absorption, Bulk Density, Apparent Porosity, and Apparent Specific Gravity of Fired Whiteware Products", 1999.
- [8] "Powder Metal Technologies and Applications", Vol.7,ASM HandBook,ASM International, 1998.

7. Nomenclature

A list of symbols are given with a brief description and unit used

Latin Symbols

Symbols	Definition	Unit
B	Bulk Density	g/cm^3
D	Dry Mass of the Samples	g
M	Saturated Mass of samples	g
m	Green Mass of Compacts	g
P	Apparent Porosity	—
P/M	Powder Metallurgy	—
S	Mass of Samples While Suspended in Water	g
V	Volume of the Compacts	cm^3

Greek Symbols

Symbols	Definition	Unit
ρ	Density	g/cm^3

Subscripts

Symbols	Definition
g	Green
op	Open Pores
Ip	Impervious portions